Fast-scale network dynamics in human cortex have specific spectral covariance patterns

Zachary V. Freudenburg[a,b], Charles M. Gaona[c], Mohit Sharma[c], David T. Bundy[c], Jonathan D. Breshears[d], Robert B. Pless[b], and Eric C. Leuthardt[c,d,1]

[a]Departments of Neurology and Neurosurgery, University Medical Center Utrecht-Rudolf Magnus Institute, 3584 CX, Utrecht, The Netherlands; and Departments of [b]Computer Science, [c]Biomedical Engineering, and [d]Neurological Surgery, Washington University, St. Louis, MO, 63130

Edited* by Marcus E. Raichle, Washington University, St. Louis, MO, and approved February 18, 2014 (received for review July 6, 2013)

Whether measured by MRI or direct cortical physiology, infraslow rhythms have defined state invariant cortical networks. The time scales of this functional architecture, however, are unlikely to be able to accommodate the more rapid cortical dynamics necessary for an active cognitive task. Using invasively monitored epileptic patients as a research model, we tested the hypothesis that faster frequencies would spectrally bind regions of cortex as a transient mechanism to enable fast network interactions during the performance of a simple hear-and-repeat speech task. We term these short-lived spectrally covariant networks functional spectral networks (FSNs). We evaluated whether spectrally covariant regions of cortex, which were unique in their spectral signatures, provided a higher degree of task-related information than any single site showing more classic physiologic responses (i.e., single-site amplitude modulation). Taken together, our results showing that FSNs are a more sensitive measure of task-related brain activation and are better able to discern phonemic content strongly support the concept of spectrally encoded interactions in cortex. Moreover, these findings that specific linguistic information is represented in FSNs that have broad anatomic topographies support a more distributed model of cortical processing.

electrocorticography | oscillating electrical potential | covariant amplitude response

The brain's intrinsic functional architecture of correlated fluctuations in resting state metabolic and electrophysiologic activity has been well established (1, 2). This functional architecture has been shown to be present in the absence of a task, during all stages of sleep, and even under anesthesia (3). How anatomically distributed regions of cortex interact during the performance of a cognitive task is less understood. Due to slower time scales associated with the hemodynamic response of current neuroimaging techniques (4) and their electrophysiologic correlates (1), the more static networks are not adequate to accommodate the more rapid dynamics associated with many behavioral tasks. Given the limitations of the described time scales, we hypothesized that faster frequencies would "spectrally bind" regions of cortex as a transient mechanism to enable fast network interactions that accommodate the flexible use of neuronal resources. Beyond previously described notions that single higher-frequency synchronization enables neuronal interactions (5), we postulated that dynamic networks are represented by a multitude of spectral characteristics. These transient spectrally covariant networks, which we term functional spectral networks (FSNs), would enable a higher level of fidelity in the transmission of cortical-cortical information.

Using invasively monitored epileptic patients as a research model, we tested this hypothesis in the setting of a simple hear-and-repeat task. Given that human speech processing involves a widely distributed area located predominantly in perisylvian regions (6), this provided a robust model to evaluate network-derived behavior. We evaluated whether spectrally covariant regions of cortex, which were unique in their spectral signatures, provided a higher degree of task-related information than any single site showing more classic physiologic responses. To minimize the impact of ictal/peri-ictal-induced alterations in cortical coherence (7, 8), all patients had normal speech function, their seizure onset zone was distinct from stimulation-defined speech areas, and testing was done on days without seizures. Taken together, our results showing that FSNs are a more sensitive measure of task-related brain activation and are better able to discern phonemic content strongly support the concept of spectrally encoded interactions in cortex. Moreover, these findings showing that specific linguistic information is represented in FSNs that have broad anatomic topographies supports a more distributed model of cortical processing.

Results

Hear-and-Repeat Task. Electrocorticographic (ECoG) data were measured from five invasively monitored human subjects with intractable epilepsy (see Table S1 for subject demographics) who underwent temporary placement of perisylvian intracranial electrode arrays to localize their seizure foci (Fig. 1 and Table S1). The subjects performed a hear-and-repeat task in which they heard a set of 36 stimuli (Fig. S1*A*). Stimuli were monosyllabic consonant-vowel-consonant (CVC) English words that were presented with 4.5-s pauses between presentations (baseline). There were four sets of nine words that had one out of four vowel sounds, the set of which collectively spanned the vowel articulation space: [i], [ɛ], [æ], and [u] (e.g., beet, bet, bat, boot). A task was chosen that allowed for two levels of granularity when distinguishing mental tasks: a general level to discriminate between speaking (task) vs. rest and a finer-grained level to discriminate between the speaking of different categories of words (subtask).

Significance

How different cortical regions are coordinated during a cognitive task is fundamentally important to understanding brain function. At rest, the brain is subdivided into different functional networks that are bound together at very slow oscillating time scales. Less is understood about how this networked behavior operates during the brief moments of a cognitive operation. By recording brain signals directly from the surface of the human brain, we find that, when performing a simple speech task, broad cortical regions are transiently bound together by shared patterns of brain oscillations that are frequency specific. In addition to demonstrating that cortical areas are broadly networked, these findings provide a new analytic tool for understanding fast-scale dynamics in the brain.

Author contributions: E.C.L. designed research; Z.V.F., C.M.G., M.S., D.T.B., J.D.B., and E.C.L. performed research; Z.V.F. contributed new reagents/analytic tools; Z.V.F. and E.C.L. analyzed data; and Z.V.F., R.B.P., and E.C.L. wrote the paper.

Conflict of interest statement: E.C.L. owns stock in Neurolutions.

*This Direct Submission article had a prearranged editor.

Freely available online through the PNAS open access option.

[1]To whom correspondence should be addressed. E-mail: LeuthardtE@wudosis.wustl.edu.

This article contains supporting information online at www.pnas.org/lookup/suppl/doi:10.1073/pnas.1311716111/-/DCSupplemental.

www.pnas.org/cgi/doi/10.1073/pnas.1311716111

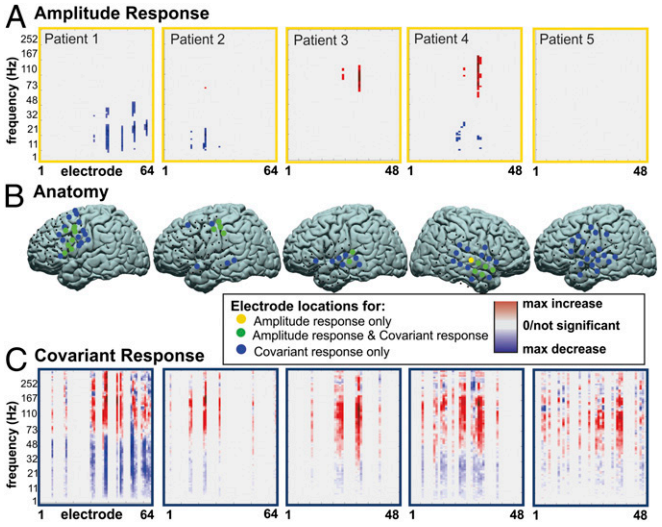

Fig. 1. Amplitude response vs. covariant amplitude response for any spoken word vs. rest for subjects 1–5 (rows 1–5, respectively) at the time period containing the voice onset time. (*A*) Thresholded ($P < 0.05$) electrode vs. frequency signed r^2 values (with red indicating a positive and blue a negative r^2 value). (*B*) Locations of the electrodes with at least one frequency bin with a significant r^2 value in amplitude response (yellow circles), the electrodes included in the FSN (blue circles), or both (green circles). (*C*) The right column shows FSN patterns in electrode vs. frequency, with small to large increases and decreases indicated with light to dark red and blue.

To best match across multiple trials the ECoG signals that correspond to the speech response, the analysis used voice onset time (VOT) to align the timing of spectral response. Each trial of the speech task was then broken down into overlapping 167-ms temporal segments with respect to the onset of the recorded speech response (Fig. S1*B* and Table S2). The mean VOT across subjects was 928 ms (SD = 459 ms) after the start of the audio stimulus. The voiced responses were generally less than 500 ms, leaving around 2.5 s of silence before the subsequent auditory stimulus. These statistics are on the same order of magnitude as those from studies using similar tasks (9) and indicate that the subjects did not have difficulty performing the experimental tasks.

Presence of Functional Spectral Networks and Topographic Distributions. Prior studies in humans using ECoG recordings have demonstrated that amplitude changes reflect cortical activation associated with a given cognitive task. Typically these are associated with a statistically significant decrease in amplitude in the lower frequencies (i.e., mu and beta) and an increase in amplitude in the higher frequencies (gamma) (10, 11). We hypothesized that, in addition to traditional amplitude responses, there are also functionally relevant covariant amplitude responses. Although there may not be a notable increase or decrease in the amplitude at a given frequency, the covariance of that amplitude modulation between sites may be significantly correlated with a task. It is these functionally relevant alterations in covariance of amplitude modulation that we term FSNs. In Fig. 1, four of the five subjects demonstrated a statistically significant amplitude change in the temporal segments just before VOT when the task of speaking was compared with rest. All five subjects, however, demonstrated a change in covariant amplitude modulation. There was anatomic overlap between the two measures of physiologic activity. The majority of electrodes that showed a significant change in power also showed a significant covariant amplitude response. Notable differences, however, are that the changes in covariance of amplitude were much broader with regard to both anatomic and frequency distribution. In Fig. 2*A*, there was a larger anatomic distribution associated with FSNs (as measured by the percentage of the electrode with statistically significant physiologic alteration) than was observed with amplitude response. This larger distribution was the case for both speaking (task) vs. rest comparisons and phoneme vs. phoneme (subtask) comparisons. The frequency bands associated with these cortical responses were also summated across subjects into a pseudospectrum across the task (Fig. 2*B*) and at different time intervals (Fig. S2). For the summated amplitude response, there are relatively classic frequency distributions associated with increases and decreases in the low and high frequencies. FSNs, however, involve amplitudes that are covariant across a much broader range of frequencies.

Timing of Functional Spectral Network Activation Relative to Amplitude Modulation. For temporal analysis, the 3-s interval from 1 s before to 2 s after VOT was broken up into 37 overlapping temporal segments or periods in steps of 83 ms. Trials for which a clear and distinct VOT time could not be defined (due to either a lack of clear overt speech production by the subject or contamination from utterances of speech that were not part of the task) were not considered (14.5%). Each temporal block from all speech trials was compared with the 0.5-s interval before the auditory stimulus and on average 2 s after the completion of the previous spoken word. Fig. 3*A* summarizes the statistically significant discriminative results [as defined by Monte Carlo (MC) analysis] for the speaking vs. rest condition for all five subjects across the amplitude response (AR) and FSN response. The data show that FSNs became significant earlier in the task and remained significant longer than the ARs of specific frequency bands at specific anatomic sites. In all subjects (rows 1–5), there are time periods showing discrimination between tasks starting ~0.5 s before the VOT and lasting up to 2 s after the VOT. The onset times of significance for the FSNs were significantly earlier than the onset times of the amplitude changes (mean, 2.6 time periods or 434 ms; pairwise $P < 0.01$), and the end times were significantly later (mean, 3.2 time periods or 534 ms; pairwise $P < 0.05$). The earlier onset and later end periods lead to the length of total time periods that are significantly detected as active speech events being significantly (pairwise $P < 0.05$) longer for FSNs. Also note that Figs. 1*A* and 3*A* indicate that, for subject 5 at the VOT, there were no significant amplitude changes. That the r^2 values for this subject are generally low indicates that ARs for this subject were relatively weak, possibly due to a low task participation level. Despite this, however, there is still a wider temporal range of significant FSNs supporting that the spectrally bound interactions were better able to capture the more subtle

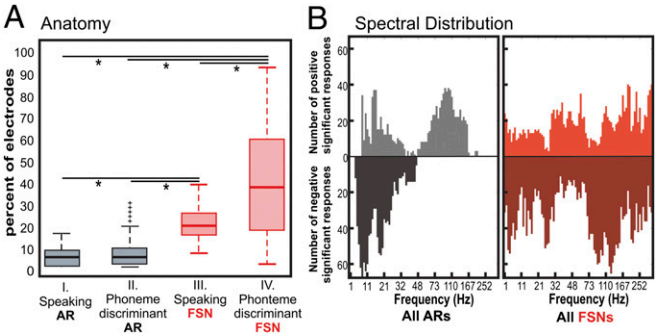

Fig. 2. Anatomic and spectral distribution of physiologic response over all subjects and significant time periods. (*A*) Distribution of the percentages of electrodes with a significant amplitude response (AR) for speaking vs. rest (I.), AR for any phoneme comparison (II.), within a FSN for speaking vs. rest (III.), and FSN for any phoneme comparison (IV.). *$P < 0.0001$. Boxes represent upper and lower quartile of data; whiskers represent maxima and minima of data. +, outlier data points. (*B*) Summated pseudospectra for ARs (gray shaded areas; *Left*) and FSNs (red shaded areas; *Right*) with significant increases (above zero line) or decreases (below zero line) over all task comparisons. Significant ARs had $P < 0.05$, and significant FSNs frequency bins had a SE above or below zero for all of the electrodes in a single spectral grouping.

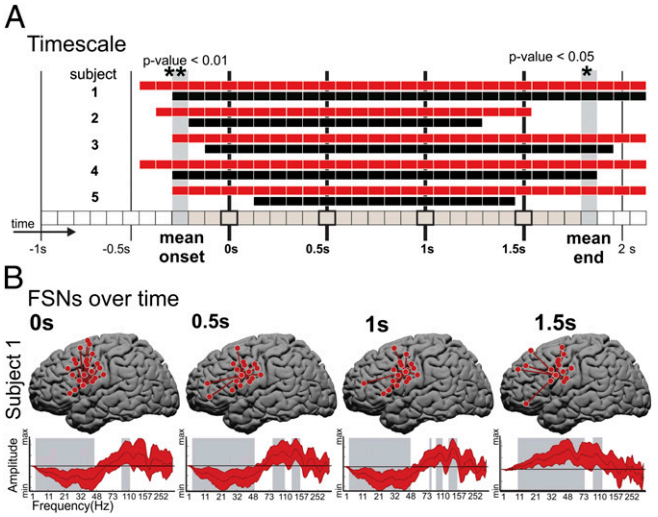

Fig. 3. Temporal characteristics. (*A*) Significant speaking vs. rest time periods for subjects 1–5 (top to bottom rows). Time points with a significant AR and/or FSN are indicated by black and red rectangles, respectively. The vertical black lines indicate the time periods that include the –1-, –0.5-, 0-, 0.5-, 1-, 1.5-, and 2-s time samples relative to voice onset time. The mean onset and end times of significance across ARs and FSNs and all subjects are indicated by the gray-shaded vertical columns. (*B*) The speech vs. rest FSNs for time periods that include the 0-, 0.5-, 1-, and 1.5-s time samples (columns from left to right) for subject 1. Each plot shows the locations on the brain and spectral distributions of the electrodes in the FSNs. The patterns represent amplitude modulations (increases or decreases) that are shared across the electrode group (as shown by the star plots) that are consistent during task when compared against rest. The shaded gray regions indicate spectral ranges with a SE within the spectral group electrode above or below zero.

physiologic responses than what was reflected by single-site frequency amplitude changes. It is important to note that, although at a given point in time the topography and spectral characteristics of an FSN are broad and more sensitive to the task than amplitude modulation, the networks are also dynamic in their characteristics. Fig. 3*B* shows the changing topographies and their spectral characteristics at VOT and at 0.5 s after, 1 s after, and 1.5 s after VOT for subject 1 (see Fig. S3 for all subjects).

Distinct Functional Spectral Network Response to Task and Subtask. Because the cognitive task was structured to look at both the broad cognitive operation (speaking vs. rest) and at different information within the broad cognitive operation (different phonemes), one could then evaluate whether there were different FSN responses between the general task (vs. rest) and the subtasks (one subtask vs. other subtasks) in the experimental paradigm. An exemplar of an FSN response across these task and subtask levels is shown in Fig. 4. Fig. 4*A* demonstrates a covariant response seen when all articulations are compared against rest. The strongest level of covariance is seen in the higher gamma ranges (~70–100 Hz). When comparing phonemic content for the different utterances, there are several notable features. Typically several FSNs are present that are necessary to distinguish between subtasks; exemplars are shown in Fig. 4 *B* and *C*. Across all subjects, distinguishing between the general task and rest largely required a single FSN, whereas distinguishing subtasks had a mean of two FSNs. Also, consistent with previous studies demonstrating that amplitude modulation in narrow-band higher-frequency oscillations was associated with different aspects of a speech task (12), these more subtask-specific networks were also associated with more narrow subbands in the high gamma range. Finally, the regions involved with parsing subtasks also appear to be widely distributed across the cortex (Fig. 2*A*). All of the FSNs for all subjects are shown in Fig. S4. Taken together, these findings support that information content associated with a given speech task involved broad cortical regions beyond those typically ascribed to that task's execution and that subtask-specific information is associated with heterogeneous subbands in the higher frequency range.

Discriminating Phonemic Content Based on Amplitude and Functional Spectral Network Response. Building on the hypothesis that FSNs are physiologically relevant to a cognitive task (and subtask), it was further hypothesized that FSN responses would be better at distinguishing phonemic content of the spoken words than classically understood amplitude changes. Using an MC *P* value statistic (*Methods*), the performance of ARs was compared against amplitude covariant responses (i.e., FSN response) in their ability to discriminate the phoneme ([i], [ɛ], [æ], and [u]) of the spoken word. The MC *P* value has the advantage that the data do not need to give a Gaussian distribution of the test statistic to evaluate the significance of the test condition. Additionally, this method is comparable across different test statistics for different measurements because the same null hypothesis is tested.

Fig. 5*A* shows FSN responses discriminate more phonemes than amplitude responses across the hear-and-repeat task for all five subjects. The figure shows a grid of gray lines representing every phoneme discrimination condition for each time period for all five subjects. The total number of significant AR discriminations and FSN response discriminations are summed per subject in Fig. 5*B* and across all subjects across all time points in Fig. 5*C*. Fig. 5*A* shows that the AR and FSN responses were very transient, with different phonemes being distinguishable at different time periods. This transience was less so for amplitude changes, which more consistently discriminated a certain phoneme condition over a longer period. It is also notable that the distribution of time periods and phoneme conditions that were associated with amplitude responses were not a subset of the FSN distribution. There is only moderate overlap in terms of time periods and phoneme conditions that could be discriminated with FSNs and those that can be discriminated with amplitude responses. Only 4% of the total found amplitude response and FSNs response discriminated the same phoneme pair at the same time point. Cumulatively, Fig. 5*B* shows that FSN responses can discriminate all phoneme pairs in three of five subjects. No subjects, however, had significant ARs that discriminate all phoneme conditions. Furthermore, when a false discovery rate is considered, significant ARs differentiated phonemes in three of the five subjects, whereas FSNs accomplished

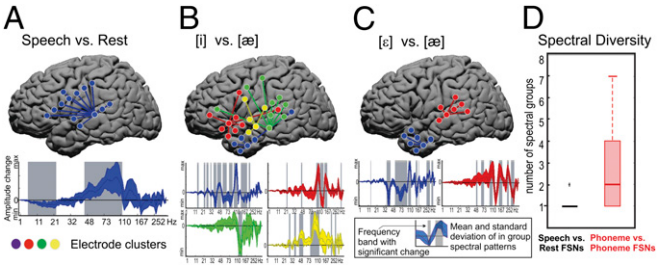

Fig. 4. FSN spectral diversity. *A*–*C* show FSNs for subject 5 and the time period from 250 to 417 ms after voice onset time. (*A*) Speech vs. rest. The top brain plot shows the locations of the electrodes included in the FSN projected onto a standardize MNI brain surface. The bottom plot shows the mean (dark blue line) and SE range (shaded blue region) of amplitude change across the spectral bins for all electrodes in the FSN. The shaded gray regions indicate spectral ranges with a SE within the spectral group electrode above or below zero. (*B*) [i] vs. [æ], with blue, red, yellow, and green indicating the four spectral groups within the FSN. (*C*) [ɛ] vs. [æ]. (*D*) Distributions of number of spectral groups in all speech vs. rest (black) and all phoneme-discriminant (red) FSNs. Boxes represent upper and lower quartile of data; whiskers represent maxima and minima of data. +, outlier data points.

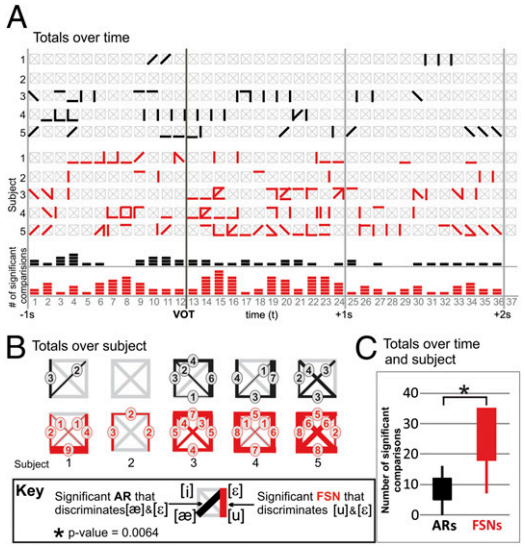

Fig. 5. Phoneme discrimination for AR vs. FSN. (*A*) Graph of time periods (horizontal axis) with significant AR (black) and FSN (red) phoneme discrimination. Rows 1–5 and 6–10 correspond to the AR and FSN results, respectively. The grids in rows 1–10 depict the six possible phoneme comparisons as described in the figure key. Rows 11 and 12 correspond to the AR and FSN results summed over subjects and phoneme pairs for each time period. (*B*) Histograms of AR (top row) and FSN (bottom row) phoneme pair discrimination for subjects 1–5. Each plot indicates the number of significant time periods between each for the six phoneme comparisons, with no significant time periods marked with a gray line. (*C*) Distributions of the number of significant time periods for ARs and FSNs summed over subjects. VOT, voice onset time.

a significant number of discriminations in all subjects. Fig. 5*C* shows that the difference in number of significant time periods for discriminating phonemes between amplitude and FSN responses was statistically significant (pairwise $P < 0.01$) on group analysis.

Discussion

This study used directly measured electrophysiologic signals recorded from the human cortex to characterize the dynamic networked behavior during the performance of an auditory-cued verbal repetition task. Functionally relevant covariant ARs, termed FSNs, were found that were associated with both the cognitive task (speaking) and subtask (phoneme). Compared with ARs alone, FSNs demonstrated earlier and more prolonged activations over broader areas of the cortex. FSNs were also superior in distinguishing phonemic content of the spoken word. These findings provide evidence for multispectral binding across cortex that is relevant to a cognitive operation in humans. Taken together, the study provides a unique approach for analyzing and understanding cortical–cortical interactions.

Historically, an alteration in amplitude of a signal has been extensively used to understand human cortical physiology. The brain generates oscillating electrical potentials over a broad range of frequencies that show characteristic task-related changes. Often described in the context of sensorimotor cortical activations, low frequencies in mu (8–12 Hz) and beta (12–30 Hz) ranges decrease in amplitude in association with actual or imagined movement, whereas higher-frequency gamma rhythms (>30 Hz) typically increase. Low-frequency modulations have broad cortical topographies, whereas higher frequencies tend to be more anatomically constrained (10, 11). It has been proposed that these low frequencies serve a more nonspecific modulatory role, whereas the higher frequencies are associated with smaller cortical ensembles and thus carry more information on a given cognitive operation (13). Although these studies do provide evidence for the information-bearing content of high-frequency amplitude modulations, they do so for discrete cortical locations. Namely, these types of analyses evaluate the correlations of amplitude modulations on an electrode-by-electrode basis. These studies do not take into account interactions between different sites. In this study, we find that, although the amplitude is important for describing cortical physiology, the manner in which amplitude covaries between sites is equal if not superior in describing the cognitive operation. This superiority is demonstrated in the earlier detections of a statistically significant signal with the general performance of the word repetition task and the improved ability to discern different phonemic content in the words that are spoken. Moreover, the frequency scale associated with this covariance appears to span both low- and high-frequency spectra. Thus, low-frequency amplitude modulation, although not substantially informative at a single site (as previously reported), does contribute on the specifics of a cognitive operation from a multisite network perspective.

There has been substantial work done in evaluating different frequency–frequency interactions that merit description in the context of this work. When considering phase-power coupling as described by Canolty et al., Canolty and Knight, and Lisman and Jensen, a lower-frequency (e.g., theta) time series consistently entrains the amplitude of a higher-frequency (e.g., gamma) series (14–16). This relationship is typically identified at the same recording site. With FSNs, the interaction is amplitude modulation that covaries with amplitude modulation (across a number of sites and across a number of frequency bands). Whereas the work of Knight and coworkers (14) identifies the important hierarchical nesting of a lower-frequency physiology to a higher-frequency physiology at a given site and infers this to represent a mechanism of binding of neural populations in a given region, our work in contrast demonstrates multisite comodulation across distinct frequency bands. This comodulation does not represent a hierarchical organization; rather, it represents a distributed binding of topographically distinct neural ensembles. The added spectral specificity of these interactions could enhance the complexity of cortical–cortical communication. The spectral specificity of interactions between two regions can enable both inhibitory and facilitating stimuli for communication concurrently, thus allowing subpopulations in a cortical region to differentially interact. Much akin to frequency division multiplexing (FDM) in communication systems (e.g., cable television), several different digital signals can be combined in a single medium (e.g., cable) by sending the signals in distinct frequency ranges (e.g., channels). Similarly, having spectrally specific characteristics that are shared between different cortical regions may facilitate optimal information exchange of shared cortical resources.

Beyond the importance of amplitude covariance as an improved methodological approach, the study provides mechanistic insights into cortical function. First, the findings support that cortical processing is substantially distributed. In previous works associated with phonemic processing, relatively constrained cortical regions have typically been identified in inferior frontal regions (17, 18). Counter to these functional imaging findings, this study showed that the cortical changes associated with differentiating phonemic content were widely spread across the cortex. A key difference between a number of the previous studies and this one is that, although numerous phonemic/phonological categories were averaged across one another to find a localized activation [e.g., phonemic monitoring (19) or phonemic segmentation (20)], we compare a specific phoneme against another specific phoneme to find their cortical representations. Thus, these findings would suggest that rather than a region, such as BA 44, being exclusively responsible for phonologic processing, these previously described localized areas are perhaps either the hub for which information is transited across the cortex or possibly the area of most common overlap.

Although the anatomic distribution of cortical interactions is broader than what is typically described with amplitude modulation, the temporal nature of these covariant responses is more constrained in time scale. The transient nature of FSNs and their

varied anatomic distributions are distinct from the more stable topographies identified with resting state functional MRI and its physiologic correlate of infra-slow cortical rhythms (1). This difference may reflect complementary physiologic roles. The slower rhythms, which can persist through sleep and anesthesia, likely reflect a mechanism for synaptic homeostasis that is needed to maintain a functional organization of different brain regions. The very rapid emergence and alteration of FSNs may represent the fast-scale acquisition and moment-by-moment integration of cortical populations as they are needed for a given stimulus or task. This notion complements modeling work performed by Deco and Jirsa on resting state networks (21). The authors integrated diffusion tensor imaging, neuroanatomic connectivity, and a model of spiking neurons with both stimulating and inhibiting synapses. They found that experimentally observed functional connectivity in humans best fits the quantitative model when the brain network operates at the edge of instability. Under these conditions, the slowly fluctuating resting state networks emerge as structured noise fluctuations around the stable low activity state induced by the presence of latent "ghost" multistable attractors. From this, they posit that there exists a multitude of available brain states in a repertoire that can be rapidly activated. In our work, we find transient networks of spectral comodulation that for a given subtask appear very discrete, but when averaged for the general task appear much more homogeneous spectrally. In essence, this "noisy" cortical behavior across all tasks is functionally relevant. These fluctuations around the average brain activation also in essence represent repertoire of activations. Thus, perhaps FSNs, in part, provide a more granular physiologic description of the dynamic repertoire of the brain network proposed by Deco and Jirsa (21).

There are limitations of the present study that must be addressed. First, the cortical electrophysiology of epileptic subjects may differ from that of the general population because of the presence of seizure foci and the chronic use of antiepileptics, which can alter both local and global levels of synchrony during and outside of the ictus (7, 8). By normalizing and combining the data across multiple subjects, we likely have accounted for many of these patient-specific pathologic elements. In addition, because the patients had normal speech and the cognitive task was performed on a day without seizures, the seizure focus was topographically distinct from speech sites, and the physiologic findings with FSNs were comparable to well-established amplitude modulations seen in normal subjects. The likelihood of these findings being accounted for by seizures is small, and thus, FSNs likely can be generalized to normal populations. Also, to the extent that nonspecific epilepsy-related physiologies were present, the analytic method used in this study identifies physiologic patterns associated with a task; thus, non–task-specific physiologies such as random ictal/periictal events would likely have been excluded (further discussion is provided in the *SI Text*). A second limitation is the restricted electrode coverage in each subject, which is determined entirely by clinical criteria. Thus, our findings should be interpreted only in the context of the cortical areas covered. This topographical restriction, and the variable anatomic localization of human speech areas, may also account for some of the varied network topographies for a given task across patients. Third, we base our physiologic findings on a speech task. Whether these findings are referable to other cognitive tasks and cortical regions will require further invasive electrophysiologic studies to further demonstrate whether FSNs generalize to all areas of the brain and brain function.

In conclusion, this study demonstrates that regions of the cortex demonstrate transient spectral covariance patterns, which we term FSNs, that are task relevant. FSNs are a more sensitive measure of task-related brain activations than are isolated amplitude modulations, which strongly supports the concept of spectrally encoded interactions in cortex.

Methods

ECoG Recording and Electrode Localization. The recording devices used in this study were 64- or 48-electrode grids with equally spaced rows of eight 2.3-mm-diameter electrodes with 1-cm center-to-center spacing. Biosignal amplifiers (g.USBamp; g.tec) were used to record the field potentials at a sampling frequency of 1.2 kHz with 24-bit resolution. BCI2000 software (22) was used to synchronize task cue stimulus presentation with the recorded ECoG signal and recorded microphone signal. The signal was digitally filtered between 0.1 and 500 Hz (with a notch filter between 55 and 65 Hz) for further analysis. The signal was also visually inspected, and those signals that had greater than three orders of magnitude greater than baseline were removed. A full description of the data acquisition and processing pipeline is given in *SI Text* and Fig. S5.

Calculation of the ECoG Spectral Response. The spectral response of the ECoG signals across the entire data set was calculated using a Gabor Wavelet Dictionary to best extract amplitude responses with temporal resolutions well fit to individual frequency ranges (23). A wavelet with a Gaussian envelope width at half maximum of four wavelengths was used to get the spectral response centered at each sample point of the signal for 88 frequencies sampled exponentially from the range of 1–338 Hz. The natural log of the Gabor Wavelet Dictionary amplitude response was taken as the ECoG spectral response.

Defining ARs from Spectral Responses. Standard cross-correlation coefficient (r^2) analysis was used to evaluate how consistently each frequency's spectral responses differed between the test conditions. Contiguous bands of spectrally adjacent frequencies whose power variations were statistically significant ($P < 0.05$) and that had the same direction of change (i.e., increase or decrease) during the task condition were defined as the ARs. The P value for significance was obtained by converting the r^2 by a generalized Fisher's method. No multiple comparison correction was performed at this stage because the P values were used to determine ARs and not the statistics of whether an AR significantly discriminates a cognitive task.

Defining FSNs from Spectral Responses. FSNs were defined as patterns of covariant spectral responses that discriminate the brain state of one task performance condition from another. To determine the spectral patterns that best discriminate the task conditions, discriminant function analysis (DFA) was used across the entire dataset. DFA is a method used to find a weighted pattern of time series variables that maximally discriminate the time series into specified groups (24). DFA has been shown to give optimal results when the sample sizes are on the order of 50 or less per condition (25). The manner in which DFA was applied in this work was closely related to linear discriminant analysis (LDA), which has recently been applied to classifying ECoG data based on spectral response (26). On high-dimensional data, a principal component analysis (PCA) decomposition gives a low-dimensional representation of the time series data, and it is common to use DFA in this low-dimensional space. In this low-dimensional space, discriminant functions define projection vectors of PCA coefficients that best discriminate the task conditions. FSNs were formed from these projections by computing their representations in the spatio-spectral space (spectral response over electrodes) and then analyzing the spatio-spectral patterns (such as those presented in Fig. 1*C*) for a subset of spectrally bound networks that are needed to significantly discriminate the task conditions. This analysis was done in a three-step process.

First, for each spatio-spectral discriminant function pattern, the electrode channels were clustered into channels with similar amplitude differences between cognitive tasks. The similarity between electrodes was computed as the correlation between the spectral patterns; this similarity measure was used as input to affinity propagation (27). This method is a robust clustering method for which the number of clusters does not need to be predetermined. An exemplar data point (i.e., ECoG channel or column in the spatio-spectral pattern in this context) was assigned to represent each cluster. The channel clusters form component pieces of the overall pattern of signal variation and conceptually represent the spectrally bound networks engaged by the cognitive task.

Second, each cluster's independent ability to discriminate between task conditions was evaluated. The correlation of the spatio-spectral pattern formed by an individual cluster with the spatio-spectral response of each recorded ECoG data sample was computed to form a correlation trace for each cluster. An r^2 analysis was then performed on the correlation traces for the corresponding task conditions to get a measure of task discrimination for each cluster component of the FSN.

Third, the FSNs were defined as the spatio-spectral pattern formed by the minimal set of clusters that needed to be included to reach significance (according to the MC *P* value method described later) in task condition discrimination. To get the minimal set, the clusters were ordered by their individual r^2 values. The clusters were then incrementally merged starting with the cluster with the highest value, and the r^2 value of the merged cluster was computed until significant task condition discrimination was reached.

Visualization and Quantification of the FSNs. The FSNs were visualized by first representing each cluster of electrodes included in the FSN as a star graph, where the exemplar electrode was connected to all of the other electrodes in the cluster, on the surface of the brain according to the anatomic locations of the electrodes (Figs. 3 and 4). The spectral component of each cluster was then given in the form of a plot showing the mean and SE across the electrodes in each cluster over the frequency domain (bottom colored plots of Figs. 3*B* and 4 *A*–*C*).

Using these visualizations as a conceptual basis, the anatomic and spectral content of the FSNs was quantified in three ways. First, the anatomic extent of the FSNs was quantified by the percentage of grid electrodes included in the FSN (Fig. 2*A*). Second, the spectral distribution of the FSNs was quantified by counting the spectral bands that had a significant decrease or increase in amplitude within an FSN. Frequency bands that had a mean response across an electrode cluster with a SE above or below zero (as indicated by the gray vertical highlight bars in the spectral plots of Figs. 3*B* and 4 *A*–*C*) were considered as significant. Although this does not mean that the individual frequency bands had a significant response to the task, such as with the ARs, it does allow for the quantification of the spectral ranges that were most relevant in the response to the task as defined by FSNs. By using this spectral range quantification, the spectral coverage of FSNs can be compared with that of individual ARs (Fig. 2*B*). Third, the spectral diversity of the FSNs was quantified by the number of electrode clusters included in the FSN. A larger number of spectral clusters indicate a larger number of patterns of amplitude change consistent over an area of anatomy that was significant in discriminating that task (Fig. 4*D*).

Comparing the Task Discrimination of ARs and FSNs Using the Monte Carlo *P* Value. ARs and the FSNs were compared in terms of their ability to discriminate cognitive tasks using an MC *P* value statistic. The MC *P* value has the advantage that the data do not need to give a Gaussian distribution of the test statistic to evaluate the significance of the test condition. In addition, MC *P* values are comparable across different test statistics for different measurements because the same null hypothesis is tested. This property allows for comparison of the MC *P* values computed for the FSNs to those of the ARs. A description of the MC *P* value method as it relates to neural electrophysiological data is given in Maris and Oostenveld (28).

To compute the MC *P* value, r^2 analysis was used as the test statistic to quantify the difference in the distributions of the data arising during two task conditions. The same test statistic was then computed for a large number (1,000) of random partitions of the data into two groups, referred to as the permutation distribution. The MC *P* value, for the task-based partition of the data, was computed by calculating the percentage of the test statistic values of the permutation distribution that were greater than the true test partition statistic.

For the ARs, r^2 analysis was performed on the summed amplitudes of the frequencies included in the AR. To calculate the permutation distribution of the AR r^2 values, the entire process (i.e., first defining ARs based on the r^2 values of the individual spectral frequency responses, then finding the best AR for each comparison, and finally computing the response and r^2 value of the best AR) was done for each of the 1,000 random permutations of the trials. This procedure was repeated separately for each speech task time period for each conditional comparison done.

An r^2 analysis was also performed on the FSN responses (i.e., correlation traces described previously), and this value was used as the test statistic for the FSNs. The principal component loading responses for each of the permutation distribution partitions were used to recalculate a DFA pattern in the PCA space for each random partition. Thus, a new FSN was created for each permutation partition whose projection onto the AR space was used when calculating the FSN response values for the permutation distribution. It was not necessary to redo PCA on the data for each random partition because PCA was done over the entire data set and not done with respect to any data groupings.

Additional Methodological Validations. These methods were also tested against white noise data and simulated spectral events as further detailed in *SI Text* and Fig. S6. To determine the relevance of this approach as it applies to noninvasive signals the analysis was also performed on simulated electroencephalographic data as shown in *SI Text* and Fig. S7. Finally, Subjects 1–5 had electrocortical stimulation for clinical speech and motor localization. Data for these subjects are shown in Fig. S8.

ACKNOWLEDGMENTS. This work was supported by National Institutes of Health Grant R21 CA159470-01A1 (to E.C.L.) and National Science Foundation Grant EFRI-1137211 (to E.C.L.).

1. He BJ, Snyder AZ, Zempel JM, Smyth MD, Raichle ME (2008) Electrophysiological correlates of the brain's intrinsic large-scale functional architecture. *Proc Natl Acad Sci USA* 105(41):16039–16044.
2. Biswal B, Yetkin FZ, Haughton VM, Hyde JS (1995) Functional connectivity in the motor cortex of resting human brain using echo-planar MRI. *Magn Reson Med* 34(4): 537–541.
3. Breshears JD, et al. (2010) Stable and dynamic cortical electrophysiology of induction and emergence with propofol anesthesia. *Proc Natl Acad Sci USA* 107(49):21170–21175.
4. Logothetis NK (2008) What we can do and what we cannot do with fMRI. *Nature* 453(7197):869–878.
5. Fries P, Schröder JH, Roelfsema PR, Singer W, Engel AK (2002) Oscillatory neuronal synchronization in primary visual cortex as a correlate of stimulus selection. *J Neurosci* 22(9):3739–3754.
6. Scott SK, Johnsrude IS (2003) The neuroanatomical and functional organization of speech perception. *Trends Neurosci* 26(2):100–107.
7. Mormann F, et al. (2003) Epileptic seizures are preceded by a decrease in synchronization. *Epilepsy Res* 53(3):173–185.
8. Amor F, et al. (2009) Cortical local and long-range synchronization interplay in human absence seizure initiation. *Neuroimage* 45(3):950–962.
9. Church JA, Coalson RS, Lugar HM, Petersen SE, Schlaggar BL (2008) A developmental fMRI study of reading and repetition reveals changes in phonological and visual mechanisms over age. *Cereb Cortex* 18(9):2054–2065.
10. Crone NE, et al. (1998) Functional mapping of human sensorimotor cortex with electrocorticographic spectral analysis. I. Alpha and beta event-related desynchronization. *Brain* 121(Pt 12):2271–2299.
11. Crone NE, Miglioretti DL, Gordon B, Lesser RP (1998) Functional mapping of human sensorimotor cortex with electrocorticographic spectral analysis. II. Event-related synchronization in the gamma band. *Brain* 121(Pt 12):2301–2315.
12. Gaona CM, et al. (2011) Nonuniform high-gamma (60-500 Hz) power changes dissociate cognitive task and anatomy in human cortex. *J Neurosci* 31(6):2091–2100.
13. Miller KJ, et al. (2007) Spectral changes in cortical surface potentials during motor movement. *J Neurosci* 27(9):2424–2432.
14. Canolty RT, et al. (2006) High gamma power is phase-locked to theta oscillations in human neocortex. *Science* 313(5793):1626–1628.
15. Canolty RT, Knight RT (2010) The functional role of cross-frequency coupling. *Trends Cogn Sci* 14(11):506–515.
16. Lisman JE, Jensen O (2013) The θ-γ neural code. *Neuron* 77(6):1002–1016.
17. Poldrack RA, et al. (1999) Functional specialization for semantic and phonological processing in the left inferior prefrontal cortex. *Neuroimage* 10(1):15–35.
18. Burton MW, Locasto PC, Krebs-Noble D, Gullapalli RP (2005) A systematic investigation of the functional neuroanatomy of auditory and visual phonological processing. *Neuroimage* 26(3):647–661.
19. Zatorre RJ, Evans AC, Meyer E, Gjedde A (1992) Lateralization of phonetic and pitch discrimination in speech processing. *Science* 256(5058):846–849.
20. Burton MW, Small SL, Blumstein SE (2000) The role of segmentation in phonological processing: An fMRI investigation. *J Cogn Neurosci* 12(4):679–690.
21. Deco G, Jirsa VK (2012) Ongoing cortical activity at rest: Criticality, multistability, and ghost attractors. *J Neurosci* 32(10):3366–3375.
22. Schalk G, McFarland DJ, Hinterberger T, Birbaumer N, Wolpaw JR (2004) BCI2000: A general-purpose brain-computer interface (BCI) system. *IEEE Trans Biomed Eng* 51(6): 1034–1043.
23. Göksu F, Ince NF, Tadipatri VA, Tewfik AH (2008) Classification of EEG with structural feature dictionaries in a brain computer interface. *Conf Proc IEEE Eng Med Biol Soc* 2008:1001–1004.
24. Johnson RA, Wichern DW (2002) *Applied Multivariate Statistical Analysis* (Prentice Hall, Upper Saddle River, NJ).
25. Pohar M, Blas M, Turk S (2004) Comparison of logistic regression and linear discriminant analysis: A simulation study. *Metodolski Zvezki* 1(1):143–161.
26. Wang W, et al. (2009) Human motor cortical activity recorded with Micro-ECoG electrodes, during individual finger movements. *Conf Proc IEEE Eng Med Biol Soc* 2009:586–589.
27. Frey BJ, Dueck D (2007) Clustering by passing messages between data points. *Science* 315(5814):972–976.
28. Maris E, Oostenveld R (2007) Nonparametric statistical testing of EEG- and MEG-data. *J Neurosci Methods* 164(1):177–190.